AD-A175 340 JET VANE HEAT TRANSFER MODELING(U) NAVAL POSTGRADUATE SCHOOL MONTEREY CA R H NUNN ET AL. 31 OCT 86 NPS69-86-010 1/1

UNCLASSIFIED F/G 20/4 NL

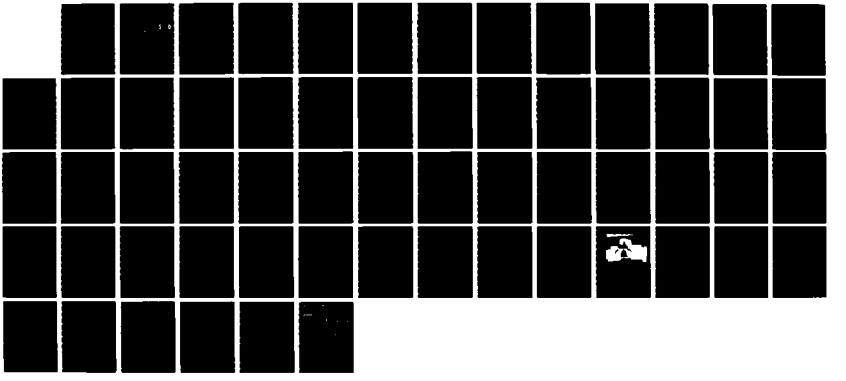

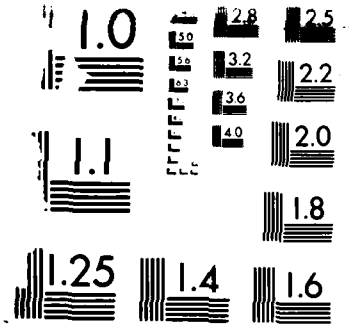
1.0
1.1
1.25
1.4
1.6
1.8
2.0
2.2
2.5
2.8
3.2
3.6
4.0

NPS69-86-010

NAVAL POSTGRADUATE SCHOOL

Monterey, California

JET VANE HEAT TRANSFER MODELING

by

Robert H. Nunn

and

Matthew D. Kelleher

Approved for public release; distribution unlimited.

Prepared for: Naval Weapons Center
China Lake, CA 93555

REPORT DOCUMENTATION PAGE

1a REPORT SECURITY CLASSIFICATION UNCLASSIFIED	1b RESTRICTIVE MARKINGS
2a SECURITY CLASSIFICATION AUTHORITY	3 DISTRIBUTION / AVAILABILITY OF REPORT Approved for Public Release Distribution unlimited
2b DECLASSIFICATION / DOWNGRADING SCHEDULE	
4 PERFORMING ORGANIZATION REPORT NUMBER(S) NPS69-86-010	5 MONITORING ORGANIZATION REPORT NUMBER(S)
6a NAME OF PERFORMING ORGANIZATION Naval Postgraduate School 6b OFFICE SYMBOL (If applicable)	7a NAME OF MONITORING ORGANIZATION Naval Weapons Center
6c ADDRESS (City, State, and ZIP Code) Monterey, California 93943-5000	7b ADDRESS (City, State, and ZIP Code) China Lake, California 93555
8a NAME OF FUNDING / SPONSORING ORGANIZATION Naval Weapons Center 8b OFFICE SYMBOL (If applicable)	9 PROCUREMENT INSTRUMENT IDENTIFICATION NUMBER N6053085WR30169
8c ADDRESS (City, State, and ZIP Code) China Lake, California 93555	10 SOURCE OF FUNDING NUMBERS PROGRAM ELEMENT NO / PROJECT NO / TASK NO / WORK UNIT ACCESSION NO

11 TITLE (Include Security Classification)
(U) Jet Vane Heat Transfer Modeling

12 PERSONAL AUTHOR(S)
Robert H. Nunn and Matthew D. Kelleher

13a TYPE OF REPORT	13b TIME COVERED	14 DATE OF REPORT (Year, Month, Day)	15 PAGE COUNT
	FROM 1Oct85 TO 30Sep 86	1986 Oct 31	54

16 SUPPLEMENTARY NOTATION

17 COSATI CODES			18 SUBJECT TERMS (Continue on reverse if necessary and identify by block number)
FIELD	GROUP	SUB-GROUP	

19 ABSTRACT (Continue on reverse if necessary and identify by block number)

A computational and experimental investigation has been undertaken to study the heat transfer characteristics of jet vanes used in thrust vector control systems. A computational model based on the PHOENICS code is being developed to predict the surface distribution of heat transfer coefficient over a jet vane immersed in a high temperature, high speed rocket exhaust. An experimental program is also being developed to verify the computational model.

20 DISTRIBUTION / AVAILABILITY OF ABSTRACT	21 ABSTRACT SECURITY CLASSIFICATION
☒ UNCLASSIFIED/UNLIMITED ☐ SAME AS RPT ☐ DTIC USERS	UNCLASSIFIED
22a NAME OF RESPONSIBLE INDIVIDUAL	22b TELEPHONE (Include Area Code) / 22c OFFICE SYMBOL

DD FORM 1473, 84 MAR 83 APR edition may be used until exhausted
All other editions are obsolete

JET VANE HEAT TRANSFER MODELING

A Report Prepared for

Naval Weapons Center

China Lake, California

by

Robert H. Nunn

and

Matthew D. Kelleher

Mechanical Engineering Department

Naval Postgraduate School

Monterey, California

October 31, 1986

ABSTRACT

A computational and experimental investigation has been undertaken to study the heat transfer characteristics of jet vanes used in thrust vector control systems. A computational model based on the PHOENICS code is being developed to predict the surface distribution of heat transfer coefficient over a jet vane immersed in a high temperature, high speed rocket exhaust. An experimental program is also being developed to verify the computational model.

Naval Postgraduate School
Monterey, California

JET VANE HEAT TRANSFER MODELLING

INTRODUCTION

Jet Vane TVC Systems

Thrust vector control (TVC) systems offer means of trajectory control that are virtually independent of external forces. Such capability is frequently required for tactical missiles, as well as spacecraft launch vehicles, when the relative flow past external lifting surfaces is insufficient to generate the necessary control forces. This commonly occurs during low-speed operations, such as at launch or during hovering flight. High angle of attack flight may also lead to regimes where conventional lifting surfaces are inadequate. In addition, there are occasions when external steering devices are infeasible from a design point of view, such as for tube-launched devices.

Several methods of TVC have been developed and applied to operational and experimental vehicles [1,2]. These include movable nozzles, internal fluid injection (secondary injection), and mechanical jet deflection systems. Jet vane systems fall in the latter category and they tend to be favored for volume-limited applications requiring relatively low actu-

ation torques and rapid response. Among the various methods of TVC, jet vanes have been found to be the most effective in delivering large thrust deflection angles (up to about 30^{o}). They may also be used with relative ease to generate roll torques.

The application of jet vane TVC dates back to the rockets designed by Goddard, and has extended to the Redstone, Sergeant, Talos, Pershing, and Algo II and III motors [1,2], as well as several intallations in smaller tactical rockets.

Of course, there are disadvantages accompanying the selection of jet vanes for TVC purposes. These include thrust losses on the order of 3-5% with undeflected vanes [2]. In addition, the attainment of relatively high thrust deflection angles may lead to axial thrust losses of the same order of magnitude as the resulting side force. However, the chief problem associated with the use of jet vanes is the large thermal loading that they experience as they are required to operate in hot, high-speed, particle-laden flows. This problem leads to design limitations so that jet vanes are often restricted to short-duration use in motors with low-temperature non-metalized propellants.

The aerodynamic (side-force producing) characteristics of jet vanes may be calculated with fair certainty on the basis of inviscid flow theory with suitable corrections for viscous effects [2,3]. On the other hand, difficulties that stem from the severity of the jet-vane thermal environment tend to lead to design practices that are based upon past experience and

cut-and-try methods. Over-design is therefore inevitable, with virtually no capacity for design optimization. In order to exploit the several advantages of jet vane TVC systems, therefore, it has become necessary to build reliable data bases and, to the extent possible, attain a fundamental understanding of the heat transfer aspects of such systems. This has led to the work reported herein.

The Jet Vane Thermofluid Environment

In the design of a jet vane system, the integrity of the vanes themselves must be guaranteed over the specified work cycle. Although this is a serious challenge, designers must also also consider the behavior of the vanes and supporting structure during transient events. Upon motor ignition, localized jet vane temperatures may rise from their initial values to near-stagnation temperatures in fractions of a second. Temperatures in the vane attachment device will rapidly follow this rise, and large thermal stresses may develop due to the proximity of a relatively cool supporting structure. These and other design aspects can only be addressed with precision if there is a good understanding of the convective heat transfer process that gives rise to the energy transfer from the flowing gases to the the vane. Put another way, the application of complex computer codes for thermal conduction in the vane and supporting structure can only follow the specification of the convective boundary conditions.

With respect to these conditions, the problem is even

more complex. The vane is immersed in a flow field that is, if generally described, compressible, turbulent, multi-component (and possibly multi-phase), three-dimensional, and unsteady, with variable properties and nonlinear and time-variant boundary conditions. These complexities, if taken more than one at a time, present a problem that is beyond the state-of-the-art for exact solution. In addition, the overall flow field will contain intersecting and impinging shock waves that give rise to discontinuous events and further complication of the boundary conditions. The presence of various protuberances only serves to exacerbate these difficulties.

To further define the problem, it may be of use to consider the levels of heat transfer that might be expected from the point of view of "simple" convection from a supersonic flow to a cooled wall. The convective heat transfer coefficient (h) may be described in terms of the nondimensional Stanton number (St) as follows:

$$h = (\ Vc_p)\ St$$

where , V, and c_p are the density, velocity, and specific heat at constant pressure of the flowing gas. On the assumption that the gas behaves ideally, this expression may be written

$$h = St\ \left(\frac{k}{k-1}\ \frac{P}{T}\ g\ I_{sp}\right)$$

where P and T are local gas pressure and temperature and I_{sp} is the specific impulse. Consider, for instance, the condi-

tions at the exit of a rocket nozzle flowing at Mach 3. With a ratio of specific heats assumed to be k = 1.2, we have, approximately:

$$h = St\ (0.25\ \frac{P_o}{T_o}\ g\ I_{sp})$$

where the subscript ($_o$) refers to stagnation conditions. If a typical case is taken to be given by P_o = 100 bar, T_o = 2560K, and I_{sp} = 250 s, then, in round numbers,

$$h = 2000\ St\ (kW/m^2K)$$

In rocket engine nozzles, a typical value for the Stanton number is about 0.002 [4]. Thus, with the result above, the expected value of the heat transfer coefficient is on the order of 4 kW/m^2K. Such a value should not be taken as conservative, since actual motor conditions may be more severe and local regions (e.g. stagnation points) may experience much higher values. By way of comparison, values of h such as these are well beyond those usually considered for convective heat transfer and, in fact, they are more typical of those realized in phase-change processes [5].

Method of Approach

In short, there can be no argument that a complete and general analytical solution is too much to hope for. On the other hand, rapid advancements in the field of computational fluid mechanics give reason to expect that much progress can be made in predicting the major features of the flow field and

their effects on heat transfer to the vane. Even so, it will be necessary to provide considerable experimental backup in order to verify numerical predictions and to evaluate the effects of factors that are beyond present-day computational capabilities.

This report describes the initial efforts in such a combined computational-experimental program. In the next section a brief review is given of some of the existing knowledge that may be brought to bear in the design of jet vane TVC systems. This is followed by a description of the code PHOENICS and discussion of some of the preliminary results that have been obtained through its use. The progress of the experimental program then will be summarized, again with some preliminary results.

BACKGROUND

This section of the report has been prepared in order to provide an overview of some of the previous work that has been accomplished in the analysis of the heat transfer aspects of supersonic flows. The particular results that are discussed are meant to prove useful as "first-cut" design guidelines for the estimation of the thermal loads applicable to the jet vane configuration. With this goal in mind, an effort has been made to identify relationships that are backed by experimental results. Purely theoretical results will not receive attention here.

It is also intended that the reference list provided will serve as a starting point for those wishing to conduct a more-complete review of the available literature. Only the unclassified open literature is discussed here, with the result that some information of a practical nature may be omitted. On the other hand, it is felt that most proven results that are widely applicable will have found their way into the public domain. For those seeking information relative to particular applications, the Chemical Propulsion Information Agency has provided a useful bibliography [6].

In searching the literature (albeit in a rather cursory way), it has been observed that relevant articles seem to be grouped in time with large intervening gaps. A surge of information appears in the mid-50s, in apparent response to stimuli provided by Sputnik and the emergence of supersonic flight as an accepted mode of transportation. The overall

impact of this work was to provide what was then seen as an adequate basis for the prediction of supersonic effects such as the aerodynamic heating of simple configurations. The complexity of the general thermal problem -- including, for instance, shock wave interactions, dissociation at high speeds, and complicated geometries resulting in three-dimensional flows -- was only accounted-for by correction factors and overdesign. Since then, with a few noteworthy exceptions, the awesome nature of the complete problem has seemingly precluded major advances in the general understanding of heat transfer in supersonic flows.

Since the mid-50s, much work has transpired in the understanding of shock wave-boundary layer interactions. Secondly, the advent of space exploration has led to significant developments in the state-of-the-art associated with hypersonic flight (with great emphasis on the space shuttle). With respect to experimental investigations, these advances have been greatly enhanced by the increasing use of facilities such as shock tunnels, gun tunnels, and Ludwieg tubes [7]. The third major factor associated with high-speed flows has been the explosive growth of the field of computational fluid mechanics. In this area, researchers are now able to predict flow effects that are most difficult, and sometimes impossible to measure with precision. From the point of view of this brief summary, neither of these latter two areas of advancement are particularly relevant.

Insofar as thermal effects are concerned, there appears

to be a relative dearth of empirical design information that is directly and generally applicable to flows at supersonic Mach numbers below about six. For flows with intact boundary layers, the results of the mid-50s still seem to be applicable, with relatively few extensions since then. We hasten to repeat, however, that this conclusion is based on a view of the literature that is far from comprehensive.

In the following discussion, initial emphasis is placed upon the thermal transport across an intact boundary layer separating a stationary flat plate from a supersonic freestream flow. Following this, some departures from this more-or-less ideal situation are discussed, such as shock wave-boundary layer interactions and the effect of suface protuberances.

Heat Transfer in Supersonic Boundary Layer Flows.

The heat transfer to or from a bounding wall occurs on a microscopic scale at the wall. The rate of heat transfer is proportional to the temperature gradient at the wall, and increases or decreases according to variations in this gradient. For given temperatures of the wall and the external freestream (outside of the boundary layer), variations in the wall temperature gradient follow variations in the freestream velocity. Increased speeds lead to thinning of the boundary layer, with the temperature change between freestream and wall occuring across the decreased thickness -- temperature gradients and attendant heat transfer rates increase with free-

stream speed, and vice-versa.

In high speed flows, these effects may be altered significantly by direct compression or viscous dissipation of energy by friction within the boundary layer. In such instances, fluid temperatures within the boundary layer may exceed freestream temperatures with attendant increases in heat transfer to a wall that is maintained below the freestream temperature. In cases where the wall temperature is maintained above the freestream temperature, heat may be first transferred <u>from</u> the wall at low speeds and then <u>to</u> the wall as the flow speed is increased.

In high speed flows, therefore, there is a certain wall temperature, above freestream temperature, at which there is no heat transfer to the wall. This temperature is called the "recovery" or "adiabatic wall" temperature. Whereas in low speed flows the freestream temperature is the reference temperature for heat transfer, the proper reference temperature in high speed flows is the recovery temperature. The recovery temperature, T_r, is defined in terms of the recover factor, r, as follows:

$$T_r = T_1[1 + r(\frac{T_o}{T_1} - 1)]$$

where the subscript $(_1)$ is used to denote conditions at the boundary layer edge. Here, T_o is the maximum freestream temperature theoretically achievable (stagnation temperature):

$$T_o = T_1(1 + \frac{k-1}{2} M_1^2)$$

so that

$$T_r = T_1(1 + r \frac{k-1}{2} M_1^2)$$

The calculation of heat transfer in high speed flows thus requires a determination of the recovery factor. The second important factor that distinquishes high speed flows from their incompressible counterparts is the fact that fluid properties are, in general, dependent upon temperature. With the severity of temperature variations in such flows, and the possibility of variations in density as well, the use of appropriate fluid properties becomes a matter of great importance.

As has been mentioned, a large amount of relevant information has been reported in the mid-50s timeframe. This is amply documented in a number of excellent review articles, among them Kaye [8], Eckert [9], and van Driest [10,11]. Applications to rocket motors are discussed in Summerfield [12] and, more recently, Ziebland and Parkinson [4]. In the following sections, we attempt to present the main features of these works.

Laminar Boundary Layers. For incompressible laminar boundary layer flow, application of the Reynolds analogy leads to a Stanton number given by:

$$St = h/ c_p V = 0.33/(Re^{1/2} Pr^{2/3})$$

It has been found that the form of this result can be carried-over into compressible flows provided that the recovery temperature, as given above in terms of recovery factor and free-

stream Mach number and temperature, is used as the reference temperature for heat transfer. That is, the heat transfer rate from the wall, per-unit-area, q'', is given by

$$q'' = h(T_w - T_r)$$

In another form,

$$q'' = h(T_w - T_1)\ [1 - f_1(r, M_1, T_w/T_1)]$$

where

$$f_1(r, M_1, T_w/T_1) = r\ \left(\frac{\frac{k-1}{2} M_1^2}{\frac{T_w}{T_1} - 1}\right)$$

which illustrates that the modification for compressible flow depends upon both M_1 and T_w/T_1.

For laminar flow, the recovery factor, and hence the recovery temperature, may be calculated with 1% accuracy by

$$r = Pr^{1/2}$$

for Prandtl numbers in the range $0.7 < Pr < 1.2$ and Mach numbers up to about 8 [8].

Use of these expressions further requires that fluid properties be evaluated at specified conditions. References [8] and [11] recommend the use of the freestream temperature for this evaluation, leading to the results shown in Fig. 1 for air with a Prandtl number assumed constant at 0.75. Note that these results lead to a value of the "constant" coefficient for the Stanton number that depends upon the Mach number and the temperature ratio in compressible flow. The question of the correct reference temperature for the evaluation of fluid properties is further addressed by Eckert [9],

in which this temperature is given the symbol T^* and is defined by:

$$\frac{T^* - T_1}{T_w - T_1} = 0.5 + 0.22\, f_1(r, M_1, T_w/T_1)$$

where f_1 is defined above.

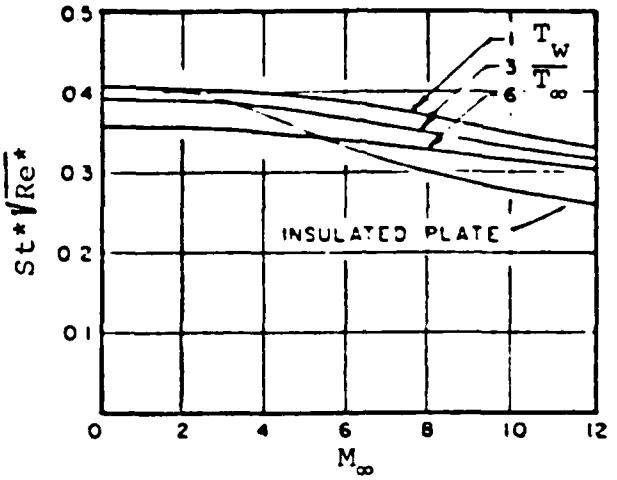

Figure 1. Local Stanton number for a flat plate in air, Pr = 0.75 [8].

In summary, for high speed flows with laminar boundary layers the Stanton number may be estimated as follows:

$$St^* = 0.33/(Re^{*1/2} Pr^{*2/3})$$

where the star notation indicates that fluid properties are to be calculated using T^*. From this, the film coefficient may be evaluated and hence the heat transfer rate per-unit-area, based upon the difference between freestream and recovery temperatures.

Turbulent Boundary Layers. The details of turbulent boundary layer flows are poorly understood -- today, as they

were in the mid-50s. Turbulent flow heat transfer formulations, based upon the Reynolds analogy between skin friction and heat transfer are, of course encumbered by the same uncertainties. With the acceptance of their approximate nature, the adaptation of incompressible formulas to compressible flows follows the same basic philosophy as for laminar flows. That is, the reference temperature for heat transfer is the recovery temperature and the fluid properties must be evaluated at T^*.

For turbulent boundary layers, the recovery factor likewise has been found to be mainly dependent upon the Prandtl number, as follows:

$$r = Pr^{1/3}$$

The resulting recommended expressions for Stanton number are

$$St^* = 0.0296/(Re^{*1/5} Pr^{*2/3}), \quad \text{for } 5\times10^5 < Re < 10^7$$

and

$$St^* = 0.185/[Pr^{*2/3} (\log_{10}Re^*)^{2.58}], \quad \text{for } Re > 10^7$$

These expressions assume a smooth plate surface. Modifications for rough surfaces are necessary, but extensive systematic information on rough surfaces exists only for the friction coefficient in low speed flows.

For both laminar and turbulent boundary layers, these expressions for high-speed flow are still recommended today for purposes of preliminary design [5].

Other Expected Features in Jet Vane Heat Transfer

The previous discussion has been related to the heat transfer associated with high speed flows with intact boundary layers in the absence of a pressure gradient. In many instances, at least locally, the boundary layer on a jet vane may be severely disrupted or even non-existent. A few references have been found that may be of use in predicting effects due to shock wave-boundary layer interactions, protuberances, and angle of attack. These are by no means the only complicating factors. Other details of the flow, which lie beyond the present coverage, include dissociation at high speeds and temperatures, surface ablation and other multi-phase multi-component effects, and boundary layer transition.

Shock Wave-Boundary Layer Interactions.

When the thermodynamic equilibrium of a substance is perturbed, the effect of the disturbance is transmitted from molecule to molecule at the speed of sound. A new state of equilibrium is reached as the thermodynamic properties adjust to the requirements imposed by the disturbance. In an otherwise uniform flow, these requirements generally arise from changes in pressure that are typically caused by a deflection of the flow at a bounding surface or by the merging of two or more streams at different pressures.

In subsonic flows, propogation of a disturbance at the speed of sound permits a gradual achievement of the new state of equilibrium in regions both upstream and downstream of the disturbance. In supersonic flows, on the other hand, fluid

elements cannot receive the disturbance "message" until they have reached or passed the source of the perturbation. While the necessary adjustments occur smoothly in a subsonic flow, they occur suddenly in supersonic flows -- instantaneously in the theoretical limit of an inviscid non-conducting gas.

Disturbances demanding large pressure decreases in a supersonic flow are accomodated by sequences of small pressure decreases, and concomittant accelerations, that may be characterized as standing wave processes that are approximately isentropic. The region of adjustment is sometimes called an "expansion fan." On the other hand, when substantial pressure increases are required of a supersonic flow, partitioning of the necessary adjustment into a sequence of smaller pressure increases reveals that associated weak waves must coalesce into a single sudden event that is characterized by its name, the "shock wave".

Substantial dissipation occurs within a shock wave and in the limit the compression and deceleration processes are mathematically as well as physically discontinuous. For these reasons, the shock wave is not isentropic and its strength is directly related to the decrease in stagnation pressure of the gas passing through it. In a perfect gas, this decrease in stagnation pressure is easily related to the entropy increase across a shock.

Flows that are at supersonic speeds relative to their surroundings cannot stay that way indefinitely. As such flows are brought to rest, either intentionally or naturally, the

attendant decelerations must be accompanied by shock wave processes. Thus shock waves are always "waiting in the wings" in supersonic flows, and the task of the designer of devices involving supersonic flows (such as rocket nozzles) is to ensure that shock processes will not be overly detrimental to performance. In supersonic diffusers, for instance, careful design can lead to gradual slowing of the flow through a series of relatively weak shocks. Thus the cumulative pressure increase is attained with less loss than that associated with a single shock process.

The strength of shock waves (usually characterized by the concomittant pressure increase) depends upon the nature of their source. In the case of the deflection of an otherwise uniform supersonic flow by a rigid boundary, shock strengths increase with the deflection angle through the range of so-called "weak waves." These waves are oblique to the flow and, in inviscid flow, they emanate from the origin of relatively small deflections. Beyond a certain maximum deflection, depending on the upstream Mach number, shock waves detach from the deflection and become curved. In such "detached shock" cases, the flow downstream of the wave is extremely complicated. The curvature of the wave converts a one-dimensional upstream flow to a two-dimensional flow, with attendant non-uniformities in Mach number (including both subsonic and supersonic regions) and thermodynamic properties downstream of the shock.

While only weak shock processes are observed when oblique

shocks are attached to a deflecting boundary, the detached shock exhibits the entire range of strengths from the normal shock, through strong and weak oblique shocks, to waves of vanishing strength far from the disturbance. In cases where boundary conditions require flow adjustments to surrounding pressures, the strengths of the shocks occuring in supersonic flows will depend upon the extent of the necessary pressure adjustment. In such free-jet flows, compressive shock processes are usually interspersed with alternating expansions, as in rocket exhaust plumes adjusting to changing atmospheric pressures.

Finally, in this brief summary, it must be mentioned that shock and expansion waves seldom occur singly and without boundaries. When these waves arrive at rigid surfaces, they are changed in strength and, in most cases, reflected. Such occurences, involving shock intersections with boundaries, are the most common instances when inviscid approximations are likely to be unjustifiable. When waves intersect with one-another, there is a mutual modulation of their strengths. Flows downstream of such intersections are generally non-uniform and likewise subject to strong viscous effects.

Heat Transfer Aspects of Shock Wave-Boundary Layer Interactions. Boundary layers are happy in the presence of pressures that decrease in the direction of flow. When pressures increase, on the other hand, the pressure force supports the shear forces already active within the boundary layer. Such increasing pressures in the flow direction impose

what is called and "adverse pressure gradient," from the point of view of the boundary layer. Adverse pressure gradients promote transition from laminar to turbulent flow within the boundary layer, as well as its eventual demise -- separation from the boundary. Shock waves are pressure increase processes that are both sudden and extreme -- there are few events that are more "adverse" as far as the boundary layer is concerned.

The boundary layer in supersonic flow is a transition region from external supersonic velocities to zero speed relative to the wall. Thus even in supersonic flow there are subsonic regions near the wall. Within these subsonic regions, it is possible to transmit pressure imbalances upstream so that the high pressures downstream of an impinging shock are felt in a region (rather than at a point) at the wall. The resulting influence on the boundary layer is more gradual than the shock process itself, and may extend for some distance along a wall. Shock impingement on a flat plate may cause separation of a laminar boundary layer, followed by reattachemt with or without transition to turbulence. Turbulent boundary layers may or may not experience local separation, depending upon the strength of the impinging shock. Figure 2 illustrates these features.

In the cases of more-complicated geometries, shock wave impingement may lead to permanent separation of the boundary layer. In any case, the effect is to greatly reduce the insulating properties of the boundary layer with local or

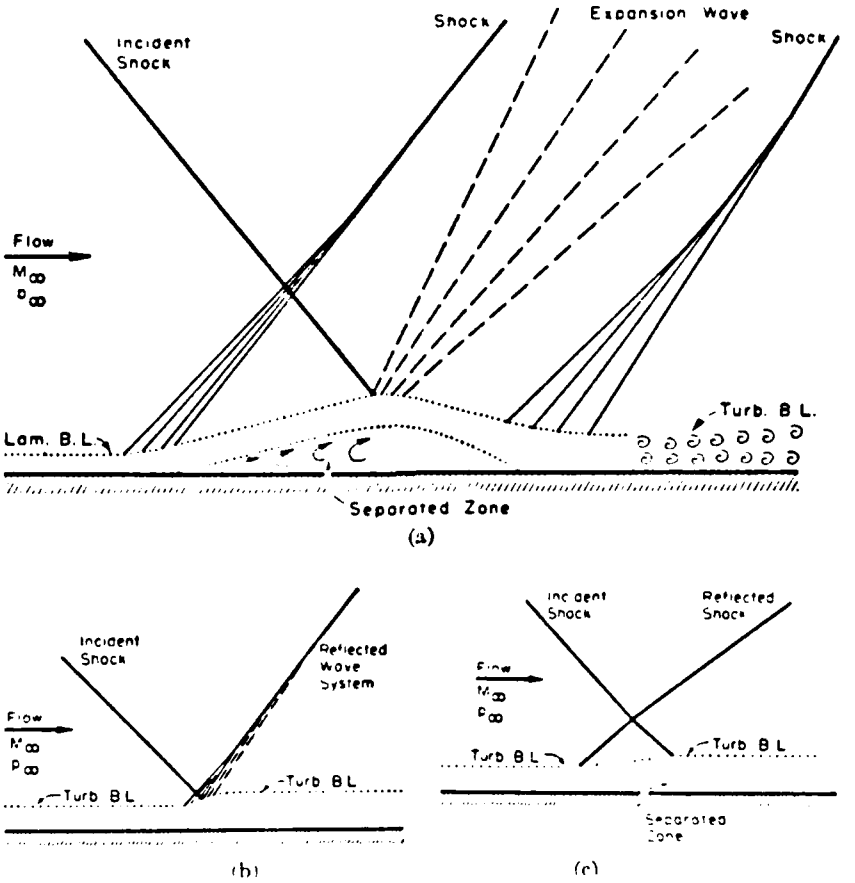

Figure 2. Examples of boundary layer behavior with an impinging oblique shock [13].

widely-spread decreases in resistance to heat transfer. Hung, et al. describe some shock wave-boundary layer effects observed in the space shuttle program [14]. Local heat transfer coefficents have been observed to be more than 100 times those observed without shock impingement. In general, the boundary interference effects can be expected to lead to increased heating rates by factors of 15 to 20.

In a jet vane system, shock wave patterns can be expected to be extremely complex. There are likely to be shock waves that emanate in the main nozzle and impinge on the vanes and

surrounding boundaries such as shrouds. These will, in turn, be reflected and secondary impingements may result. Even if the main nozzle and shroud do not generate significant shocks, the vanes will do so and these shocks may impinge on other vanes. Finally, the shock patterns will vary depending upon motor operating conditions and vane deflection angles.

From a design point of view, however, it should be sufficient to identify the worst-case shock impingement problem. This may be quite difficult but, if it is correctly done, secondary and higher-order impingements should not lead to catastrophic events. For instance, a preliminary study might be conducted to identify the origin of the strongest possible shock during a jet vane excursion. Having done this, the point of nearest possible impingement could be predicted. Such a point would be a critical point for design purposes and the local shock strength there could be used to estimate the worst-case possibility with respect to convective heat transfer.

Fortunately, there is an abundance of information in the literature that allows prediction of heat transfer amplification due to shock wave-boundary layer interaction [7, 14-16]. The most common method is to relate the ratio of heat transfer coefficients to the pressure ratio accompanying shock impingement:

$$\frac{h_{i,pk}}{h_u} = \left(\frac{p_{i,pk}}{p_u}\right)^n$$

In this expression, the subscript $(_{i,pk})$ refers to the peak

values due to impingement while the subscript ($_u$) refers to values calculated for the undisturbed boundary layer flow.

The recommended value for the exponent n varies from 0.7 to 0.85, depending upon the state of the boundary layer, with the higher value used for the turbulent case. The methods previously described are recommended for calculation of the undisturbed value of the heat transfer coefficient. It is important to note that the undisturbed pressure is not that behind the impinging shock, since the pressure rise at the surface is attenuated somewhat by the spread of the separated region. The references cited above will lead to appropriate values for the pressure ratio.

The apparent validity of the correlation between heat transfer and pressure ratios in disturbed boundary layers is most fortunate since, in most cases, it is much easier to measure pressures than heat transfer coefficients. Further information relating to practical applications in this area, including heat transfer with ablation, may be found in [16] and [17].

Protuberances. In many ways, the design configurations of jet vane systems give the impression that the vanes will appear as blunt bodies from a fluid mechanical point of view. In addition, practical designs often include structural members (fasteners, brackets, shrouds, etc.) that can appear as protuberances to oncoming supersonic flows. The nature of the interactions induced by such obstructions is basically one of a strong-shock upsetting a boundary layer.

Much work has been done in estimating the effect of protuberances in boundary layers. Relevant information, as well as further references will be found in Whitaker and Ostowari [18] and Sedney and Kitchens [19]. The latter work describes the geometry of the interaction regions for various obstacle shapes, and discusses the depen-dence of these regions on Mach number and Reynolds number.

The heat transfer implications of protuberances in discussed in Datis, et al. [20], and correlations are presented for estimating heat transfer amplifications. Highest amplifications occur usptream of protuberances, and can be as much as five-fold -- on the order of stagnation point heating. Immediately downstream, regions of reduced heat transfer have been found with relatively mild increases observed far downstream of the obstruction.

Effect of Angle of Attack. Much of the preceding discussion is only relevant to cases when the jet vanes are at relatively small angles of attack to the oncoming flow. In many instances, however, jet vane operation may occur at angles of attack up to about 30^{o}. The effect of angle of attack has been considered by Motwani, et al. [21], in a series of tests of low aspect-ratio rectangular plates at various angles of yaw and pitch in subsonic flow under turbulent boundary layer conditions.

The angle of yaw was found to have an insignificant effect upon heat transfer. The angle of attack effects were observed to be influenced by whether or not separation bubbles

were established at the leading edges of the plates. The presence of leading edge separation, together with aspect-ratio (edge flow) effects, actually led to decreases in the average film coefficient below those expected for zero angle of attack. In addition, values decreased with angle of attack at the lower angles. At angles above 30^{o}, dependency of heat transfer on angle of attack was no longer observed. It was noted, however, that the effects of increasing favorable pressure gradient with angle of attack may have been responsible for relaminarization of the flow with subsequent decreases in film coefficient.

The tests described in [21] were complicated by a number of factors, and careful analysis would be necessary to determine if these results are applicable to the jet vane problem. Expectations of decreased average heat transfer coefficient with angle of attack, based upon these results, are probably not warranted. In any case, high local heat transfer rates at leading edges are well-known occurences and, in the jet vane problem, leading-edge shocks are likely to have significant effects on the downstream boundary layer behavior. What can be said with certainty, is that further numerical and experimental work is necessary with respect to the effect of angle of attack on boundary layer flow and heat transfer.

COMPUTATIONAL MODELING

A major objective of the work undertaken is to develop a computational tool which can be used to assess the heat transfer characteristics of jet vane thrust vector control systems. As described previously, the flow environment seen by the jet vane during operation is very severe: the impinging rocket exhaust flow is supersonic, very hot, probably with some solid particles, and possibly chemically reacting. Also, from a computational point of view, the geometry of the jet vane is highly complex. Finally, the flow is not planar but is more nearly conical.

Only a few years ago the numerical analysis and calculation of such a flow field was completely impossible. In the past several years great strides have been made in the development of numerical techniques for computational fluid dynamics (CFD). The impetus for this rapid advance in CFD has been the concurrent development of today's super computers. Indeed it is arguable that the needs of modern CFD codes has been a major cause for the development of super computers. Whatever the underlying causes, we have reached the point in the development and implementation of CFD that an engineering analysis of the jet vane heat transfer problem is a real possibility.

These rapid developments in CFD are well documented in the recent books by Peyret and Taylor [22], Patankar [23], and Jaluria and Torrence [24]. The problems associated with the numerical analysis of compressible flows are covered in the

survey article by MacCormack and Lomax [25] while the compilation of papers edited by Book [26] provides a great deal of insight into the very specialized vectorizing techniques necessary to efficiently implement CFD on modern super computers.

The state of maturity of CFD is evidenced by the fact that there are now commercially available large scale general purpose computer codes for analyzing complex flow situations. Examples of these include: FLUENT and its variations from Creare Inc., in Hanover NH; FIDAP from Boeing Computer Services in Seattle, WA; and PHOENICS from CHAM of North America in Huntsville, AL. Since the task at hand was to develop an engineering analysis and design tool for assessing the heat transfer characteristics of jet vane thrust vector control systems and not to undertake an extended program of CFD code development, it was decided to use one of the commercially available codes and adapt it to the jet vane geometry and flow conditions.

Because of prior favorable experience at the Postgraduate School with earlier versions of CHAM codes it was decided to use PHOENICS to implement the computational modeling. The availability of Mr. Amiram Leitner, of the Isreali Ministry of Defense, who was spending a sabbatical year at the Postgraduate School added a note of serendipity to the choice of PHOENICS. Mr. Leitner is the leader of a software development group for the Isreali Defense Research Lab, and is an expert in the use of PHOENICS for the analysis of missile related flow problems. Mr. Leitner's expertise was invaluable in the computational modeling

effort of the past year.

Description of the PHOENICS Code

As described in the instruction manual: "PHOENICS is a general-purpose computer code for the simulation of fluid-flow, heat-transfer, mass-transfer,and combustion processes. It handles one- or two-phase flows, in one, two or three dimensions; and it can be applied to numerous problems arising in engineering, scientific research and the environment." The word PHOENICS is an acronym for Parabolic, Hyperbolic, Or Elliptic Numerical Intergration Code Series. (The reference to parabolic, hyperbolic or elliptic is to the partial differential equation class to which the Navier Stokes equations may belong depending on the magnitude of the Reynolds number and Mach number.)

Built into PHOENICS are the equations , and the corresponding computer coding sequences, which express the conservation laws of: mass of each phase present; the three components of momentum for each phase; the thermal energy of each phase; the mass concentration of each chemical species; and the fluxes of thermal radiation. Also included are turbulence models which account for the conservation of the energy and length scale of the turbulence. The equations contain individual terms which express the processes of convection, diffusion, generation and dissipation, with appropriate account taken of the interaction of turbulence with laminar flow phenomena. The conservation equations are applied to a large number of contiguous sub-domains or cells, into which the region of study is artificially devided.

The PHOENICS computer code is modular, with separate modules for input, output, computation, restart, and other computer "house keeping" chores. A more complete description of the structure of PHOENICS and its use can be found in the documentation for PHOENICS [27].

Use of PHOENICS for the NWC Jet Vane Configuration

The geometry of the NWC jet vane configuration is shown in figure 3. As is obvious the geometry of the vane is three

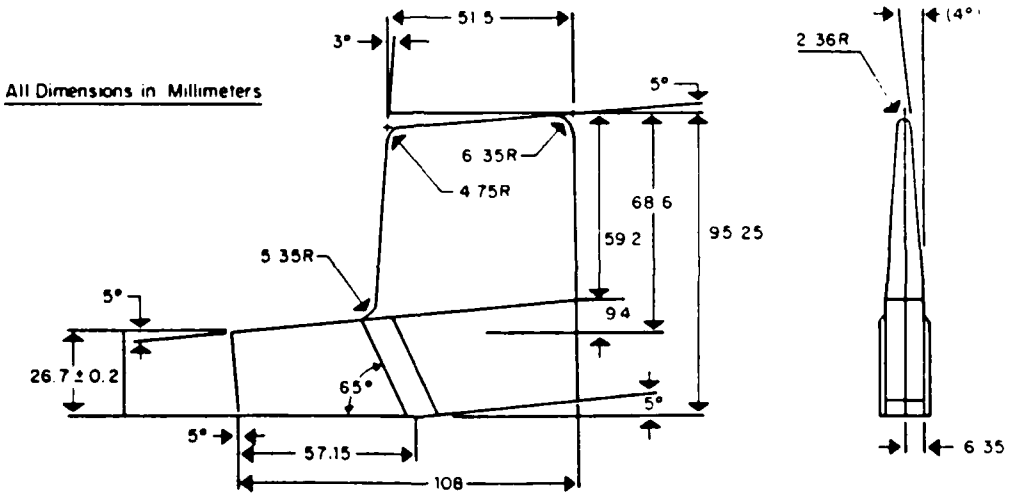

Figure 3. NWC Jet Vane Configuration

dimensional and quite complex. The modeling of such a problem is even more difficult when it is recalled that the impinging flow is conical and the vane operates at angle of attack. To gain initial familiarity with the use of the PHOENICS code and at the same time gain useful engineering information about the surface heat transfer characteristics of the vane initial two-dimensional approximations of the vane geometry were constructed.

Two approximations were used, one with a sharp leading edge and one which attempted to approximate the actual rounded leading edge of the vane. The dimensions of these two approximations are illustrated in figure 4.

All Dimensions in Millimeters

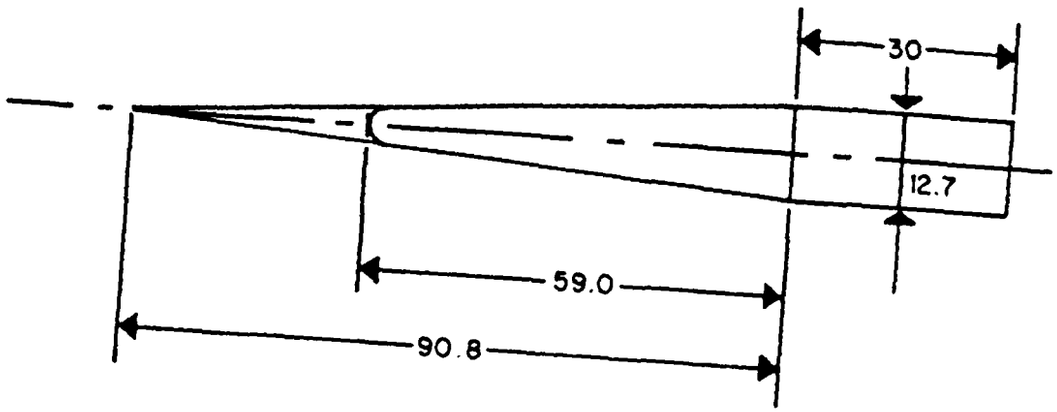

Figure 4. NWC Jet Vane Approximations

The major difficulty in numerically modeling such a complex flow situation is in constructing an appropriate finite difference grid to capture and resolve some of the complicated physical phenomena such as the viscous boundary layer over the surface, the leading edge shock wave, or the expansion waves from the shoulder and the base of the vane. The grid construction and the other details of the implementation of the PHOENICS code for the NWC jet vane approximations are completely covered in the report by Leitner [28] and the Master of Science thesis by Yukselen [29]. What will be presented here are some of the results of the PHOENICS calculations taken from these two

documents.

Results of Calculations

Four cases were calculated: sharp edge vane and blunt edge vane; laminar boundary layer and turbulent boundary layer on each vane. For all cases the free stream Mach number was 3.2. The results presented in figures 5 through 8, are given as streamwise variations of local surface shear stress coefficient (C_f), or local Stanton number (S_t). Figure 5 gives the distribution of the shear stress coefficient over both the sharp edge vane and

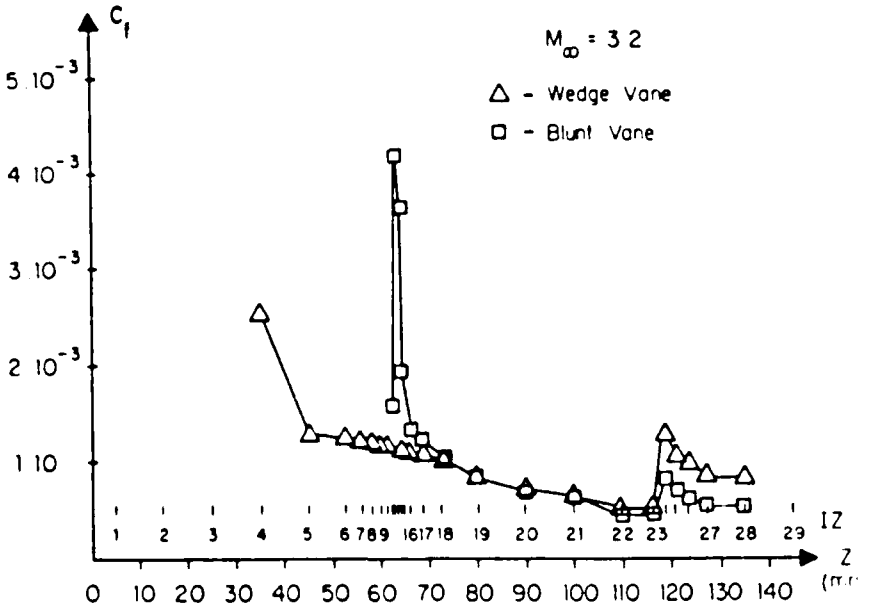

Figure 5. C_f for a Laminar Boundary Layer

the blunt vane with a laminar boundary layer. As would be expected the shear stress shows a maximum at the start of the vane and falls rapidly downstream with another jump at the shoulder of the vane. Over most of the wedge portion of both vanes the value of C_f is independent of the geometry of the leading edge. The blunt vane shows a higher initial C_f and a higher C_f at the shoulder than for the sharp edge vane. Figure 6, shows the distribution of C_f for the same two vanes with a turbulent boundary layer. The shear stress coefficient for the blunt vane starts much higher than the sharp edge vane but drops rapidly to a value significantly lower than the sharp edge vane over most of the vane surface. Figures 7 and 8 give the distribution of the local Stanton number for both vanes for both laminar and turbulent boundary layers. In both figures the trends are the same as for the C_f distributions. From these results it appears that the influence of the leading edge geometry is much more pronounced for the turbulent boundary layer than for the laminar boundary. At the high speeds and the length scales involved in these cases it is expected that the boundary layer would be turbulent.

The cross over that is observed to result due to the leading edge geometry with the turbulent boundary layer, is not fully understood at this time but numerical anomolies cannot be ruled out. The shape of the leading edge, of course, has a great effect on the rate of growth of the boundary layer and on the shape and position of the initial shock wave. It is felt that

the influence of the leading edge geometry on the shock wave is probably the more significant phenomenon in causing the observed cross over.

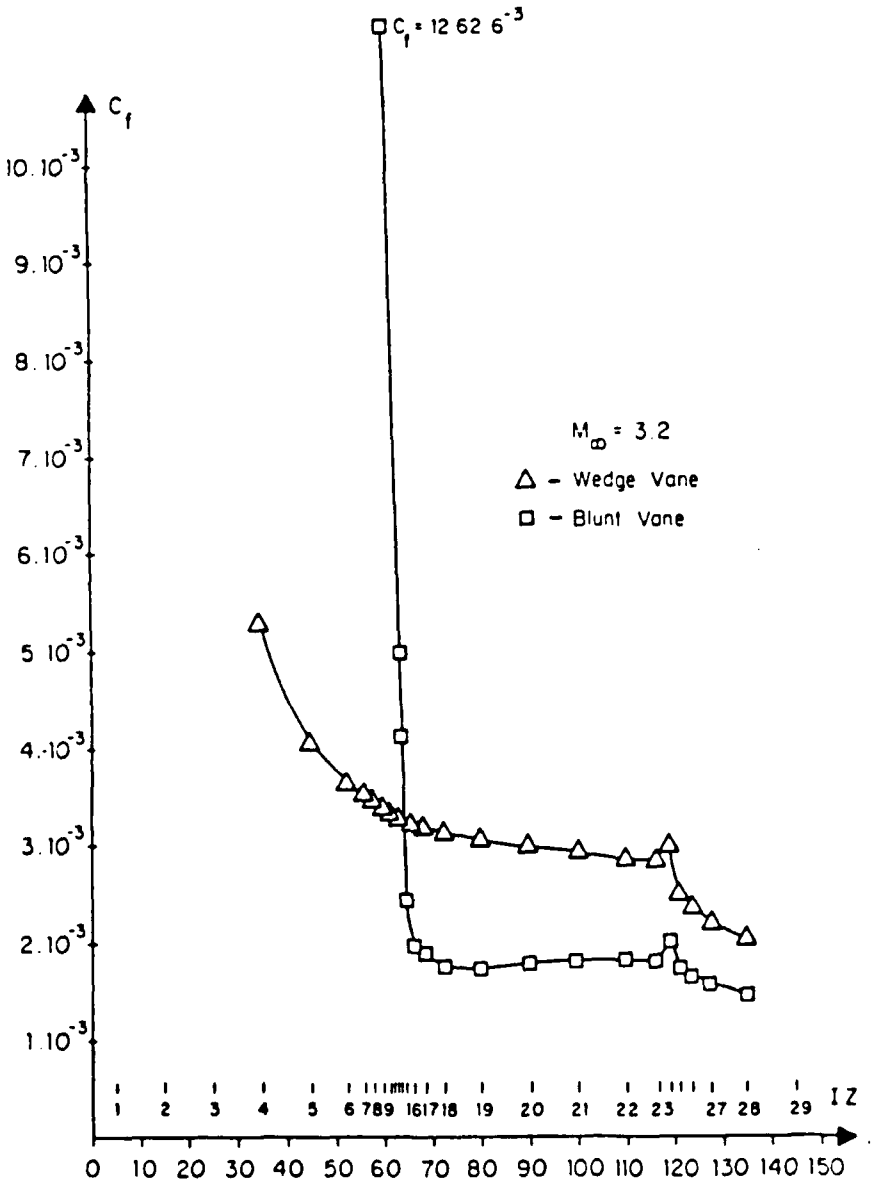

Figure 6. C_f for a Turbulent Boundary Layer

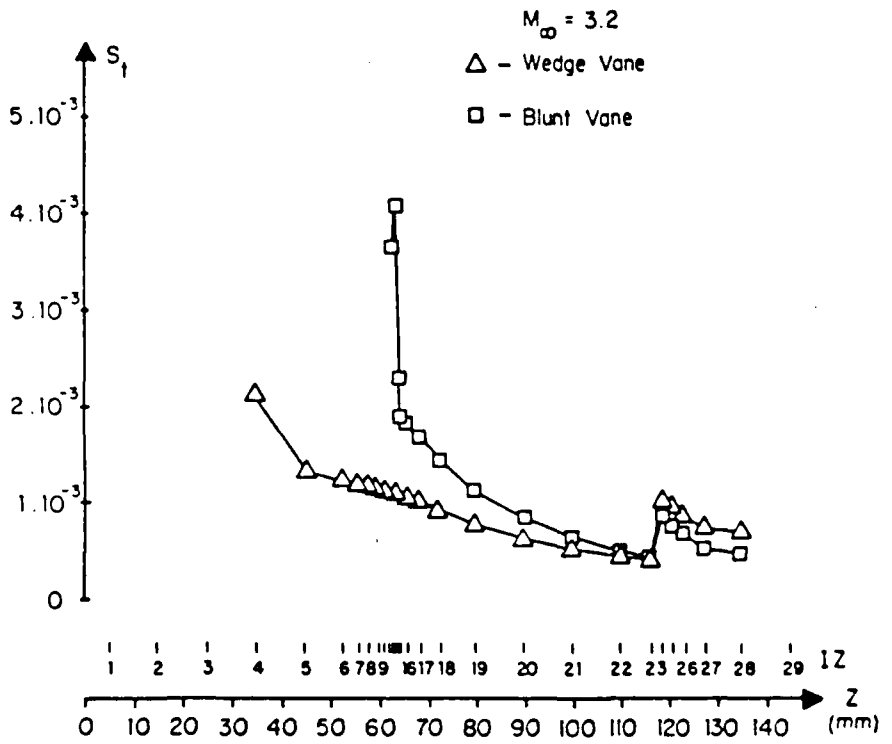

Figure 7. S_t for a Laminar Boundary Layer

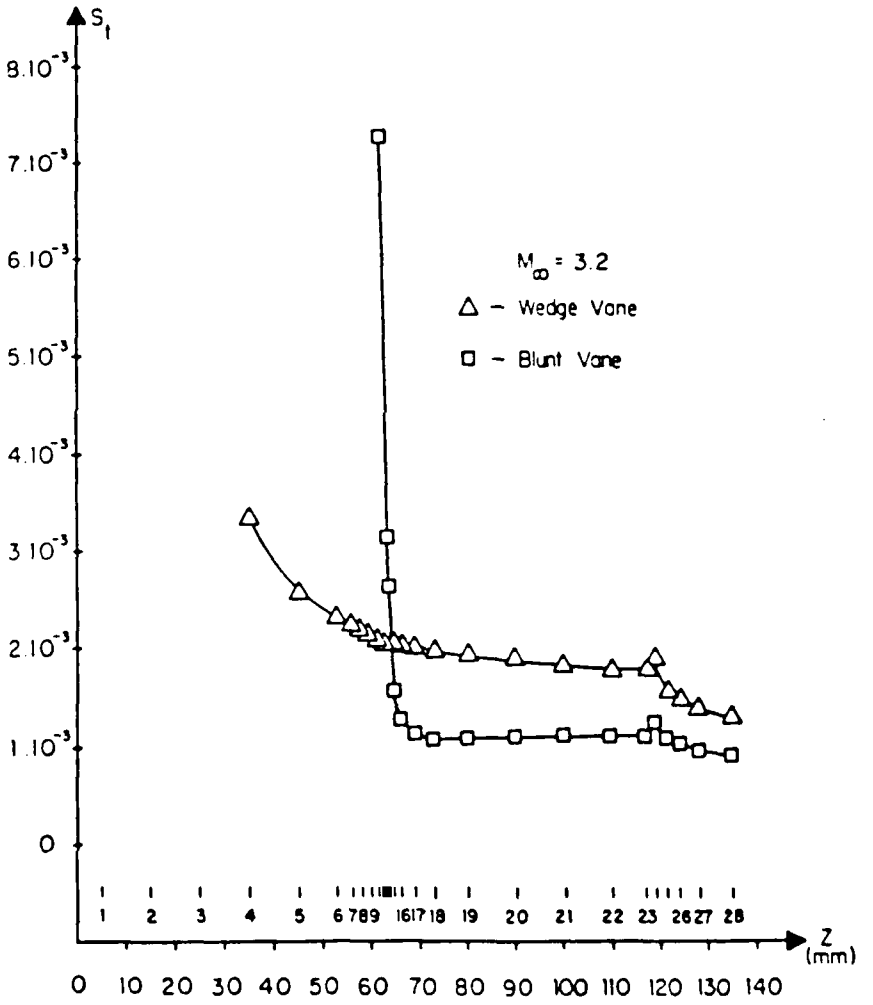

Figure 8. S_t for a Turbulent Boundary Layer

EXPERIMENTAL PROGRAM

A program of experimental investigation has been begun with two main goals in mind. These are (1) to develop a capability to experimentally evaluate the accuracy of the heat transfer predictions evolving from the CFD analyses and (2) to provide a means for estimating the effects of complicating factors that are beyond the state-of-the-art in numerical modeling of jet vane flow fields.

Two flow facilities are available at the Naval Postgraduate School to support these tests. The low-speed low-turbulence wind tunnel provides flow at speeds up to 100 m/s in a test section 1.8-m long, 0.7-m high, and 0.5-m wide. A small blow-down supersonic wind tunnel is also in place, driven by a 2.4-MPa (350 psia) supply system. The test section of this facility is approximately 10-cm square with nominal test-section Mach numbers of 1.5, 2.0, 2.8, and 4.0 attainable using interchangeable nozzle-blocks.

Heat Transfer Measurements in High-Speed Flows

The experimental deduction of convective heat transfer characteristics necessarily involves the measurement of two basic quantities: the driving temperature difference and the resulting rate of heat flow to or from the wall. Under steady state conditions, these may be measured by noting the heat flux needed to maintain the wall at a specified constant temperature in the presence of the external flow. This classical method has been extensively used for low speed flows where large test surfaces can be evaluated with relatively easy

access for the necessary instrumentation and control [5,30].

In high-speed flows, where models tend to be relatively small and inaccessible, a common method for heat transfer experimentation is the so-called transient method. In this method, models are designed with thermal characteristics such that internal resistance to heat conduction is negligible with respect to that of the convective film. In such a situation the model temperature distribution may be assumed to be relatively uniform and the major temperature gradient would be that obtained across the convective boundary layer. The resulting analytical method is one of "lumped heat capacitance" with the model taken to be a uniform temperature sink (or source) with respect to the convective boundary condition. From an energy balance for such a case, the rate of heat flow across the boundary is

$$q' = hA(T_w - T_r) = - mc \frac{dT_w}{dt}$$

where A is the convective surface area and m and c are the mass and heat capacity of the model.

Solution of this simple differential equation leads to the prediction of a wall temperature response given by

$$\frac{T_w - T_r}{T_i - T_r} = \exp\ (-t/t_c)$$

where T_i is the initial wall temperature. The time constant for the event is given by

$$1/t_c = \frac{hA}{mc}$$

This time constant may be further characterized through the use of the non-dimensional Biot and Fourier numbers:

$$Bi = hv/kA, \quad Fo = \alpha (A/v)^2 t$$

where v is the model volume and α is its thermal diffusivity. The elapsed time may now be written in terms of time constants as:

$$t/t_c = Bi \times Fo$$

The appearance of the Biot number in these expressions is particularly informative since the value of this number expresses the resistance to conduction in the model relative to the convective resistance of the external flow. According to the premise of lumped thermal capacity, the value of the Biot number must be small -- suggested limiting values are on the order of $Bi \leq 0.1$ [5, p. 101].

With experimental procedures suitably designed, the measurement of the model temperature variation with time leads to the determination of the time constant for the response and thence to the film coefficent, h. A number of practical difficulties arise, including attainment of a desired initial model temperature and the maintenance of this temperature during wind-tunnel start-up transients. If the rate of heat flow along the model is not negligible, the model temperature may become nonuniform. Errors due to this source may be minimized by short measurement periods (in which the change in model temperature does not give rise to significant streamwise temperature gradients) as well as the maintenance of small

Biot numbers.

In compressible flow, the transient method requires the calculation or measurement of the recovery temperature. If the run duration is sufficiently long, this equilibrium temperature may be extrapolated in time (providing that streamwise conduction in the model is not a factor). Measurement of local model surface temperatures may also be a problem and, in such cases, surface temperatures are often deduced by means of thermocouples imbedded within the model -- the so-called inverse conduction problem. These and other factors are discussed in Bleakney [31] and Burbank and Hodge [32]. Applications using imbedded thermocouples are developed and refined in Williams and Curry [33], Mehta [34], and Raynaud [35].

Preliminary Experimental Work.

As noted above, the experimental program has two main goals. To verify (or refute) the results of the numerical calculations, tests were designed to measure heat transfer coefficients in supersonic flows past standard shapes. For the first tests the nominal test-section Mach number was selected to be 2.8 and the model configuration was a double-wedge (diamond).

Model Design. In order to use the transient method, model design necessitates a configuration leading to the smallest possible Biot number. To do this, it becomes necessary to estimate the film coefficient for the nominal test condition.

For a double-wedge with 6-degree half-angle in Mach 2.8

flow, the freestreem Mach number downstream of the attached oblique shock is about 2.52. With nominal stagnation conditions of 0.7 MPa (100 psia) and 290 K (520 R), corresponding freestream static conditions are P_1 = 38.7 kPa (5.6 psia) and T_1 = 127 K (229 R). The freestream velocity may be calculated to be 570 m/s (1870 ft/s). For standard air properties [36], the kinematic viscosity at these freestream conditions is found to be 8.3×10^{-6} m^2/s (8.9×10^{-5} ft^2/s), with a corresponding Reynolds number per-unit-length of 2.1×10^{7} ft^{-1}. For models of the size contemplated for the small supersonic wind tunnel, this leads to Reynolds numbers on the order of 4×10^{6} -- marginal with respect to the possibility of laminar flow on the model surface.

Following the methods described earlier for compressible flow, the following values may be calculated for laminar flow at a point 5 cm along the wedge with a wall temperature of 290 K:

$$
\begin{aligned}
r &= 0.85 \\
T_r &= 211 \text{ K} \\
T^* &= 240 \text{ K} \\
Pr^* &= 0.72 \\
Re^* &= 3 \times 10^{6} \\
St^* &= 2.4 \times 10^{-4} \\
h &= 227 \text{ W/m}^2\text{K}
\end{aligned}
$$

The corresponding value for film coefficient if turbulent flow is assumed is 1780 W/m^2K. This latter value is assumed to be the most likely in actual testing and, in any event, it fixes the worst case in terms of minimum Biot number.

Copper [k = 400 W/mK (230 Btu/hr-ft-R)] was chosen as the model material. For this configuration, shown in Fig. 9, the

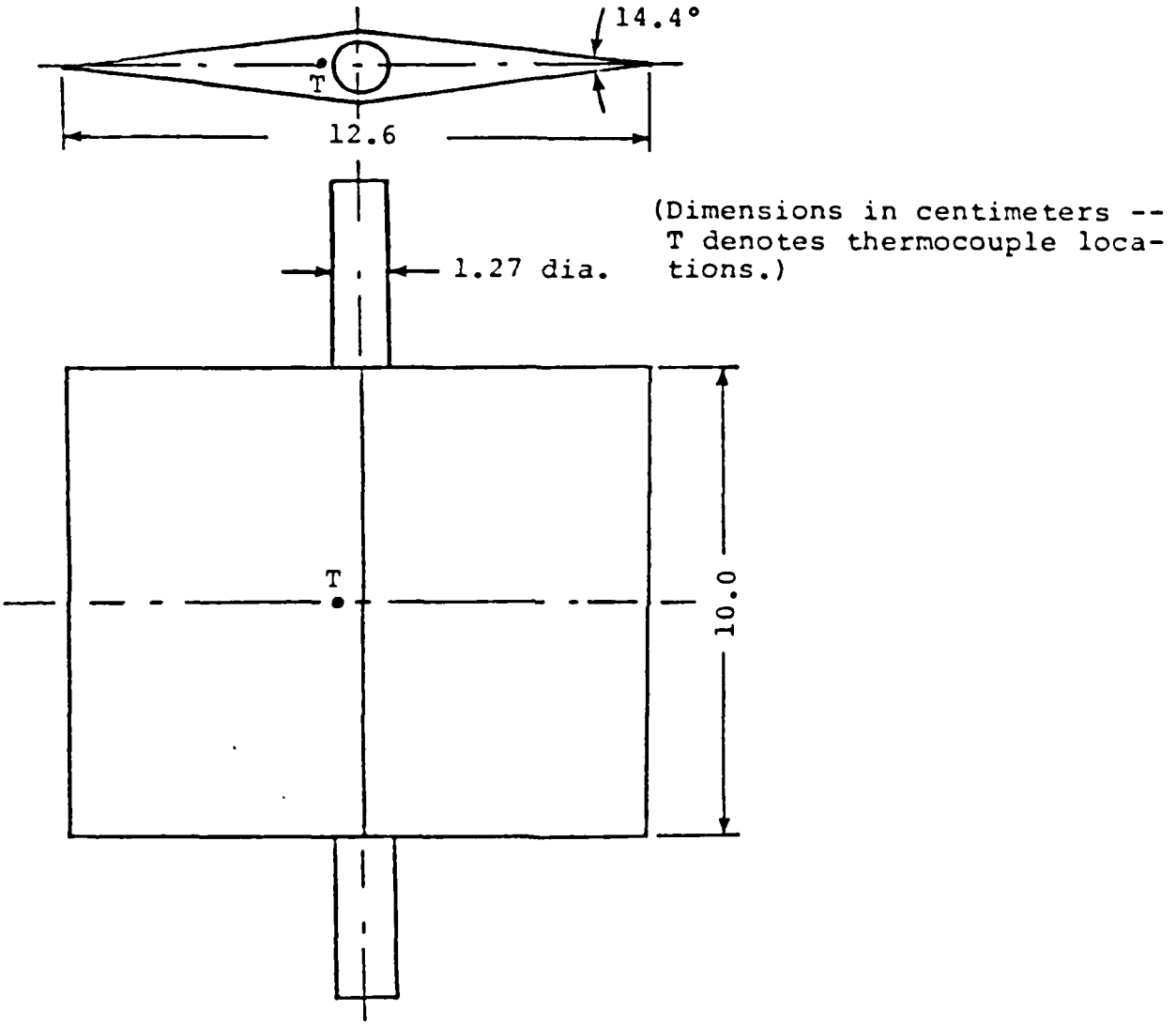

Figure 9. Sketch of wedge model.

volume-to-area ratio is $v/A = 4 \times 10^{-3}$ m and, using the turbulent value estimated above for the film coefficient, the expected nominal Biot number is about 0.018 -- well below the desired maximum.

Measurements Using Infra-red Thermography.

Application of the transient method for heat transfer experimentation requires the measurement of surface temperatures, preferably at every point of interest on the model. This presents several significant problems: (1) location of thermocouples on a surface is often difficult, and the wiring necessary may lead to interference with the thermal and flow fields, (2) response times of thermocouple temperature sensing systems may be so slow as to distort the recorded transient response, (3) prior to testing, investigators may not know what points are liable to be of particular interest -- good experimental insight and probably luck are necessary to pick up anomolous behaviors, and (4) pointwise measurements do not indicate spacial trends on the model surface -- observed effects may be due to extreme gradients not detected by a given thermocouple array.

With recent IR sensing and recording technology, these difficulties are virtually eliminated. In addition, the second goal of the experimental investigation -- to test complex jet vane geometries in various orientations -- is especially enhanced by IR thermography.

The thermal imaging system that has been employed in the experiments described below is the Probeye Thermal Video System, Series 4300 [37]. This system provides real-time temperature maps of objects through 16 color bands displayed on a color monitor and recorded on video tape. The temperature range of the system is from 233K to 553K (-40xF to 536xF) and

the 16 color bands may be selected to span all or portions of this range. Emissivity adjustments can be made from 0.0 to 1.0 in increments of 0.01, in the spectral wavelength band of 2.0 to 5.6 fm. The unit includes a movable cursor which can be placed at any location in the field of view, giving digital readout of the temperature at that location. A real-time clock gives readouts precise to 0.1 seconds.

The use of this imaging system requires employment of an optical window transparent to IR radiation in the wavelengths to be sensed. For this purpose, a six-inch diameter window, 2 mm in thickness and fabricated of magnesium fluoride has been used in experiments in the subsonic wind tunnel. This material, tradename IRTRAN 1 (Eastman Kodak Company), allows over 95% transmittance in the 2.0 to 5.8 fm range [38]. The window is capable of withstanding differential pressures of up to one atmosphere and ambient temperatures, with a safety factor of four.

Results_of_Subsonic_Tests.

Before the system for use in the supersonic wind tunnel could be designed, fabricated, and installed, this facility was deactivated pending safety tests. At the time of this writing, these tests have not yet been completed. Accordingly, the subsonic tunnel was selected in order to continue the work and to gain familiarity with the test procedures and equipment, and to develop validated methods for data acquisi- and reduction. The details of these tests are recorded in Spence [39].

The model designed for the supersonic tests was fabricated without heating provisions. Because of the accessibility of the model when mounted in the subsonic tunnel, it was possible to heat the model using a thermal blanket device that was manually removed at the instant prior to starting the tunnel.

Results for the Double-Wedge.

Following extensive testing of the details of the experimental setup and calibration of the sensing instrumentation, production runs were conducted over the range of available wind tunnel speeds. The transient method was used to reduce the data from the surface thermocouple (Fig. 9) as well as from the IR indications given with the cursor overlayed on the

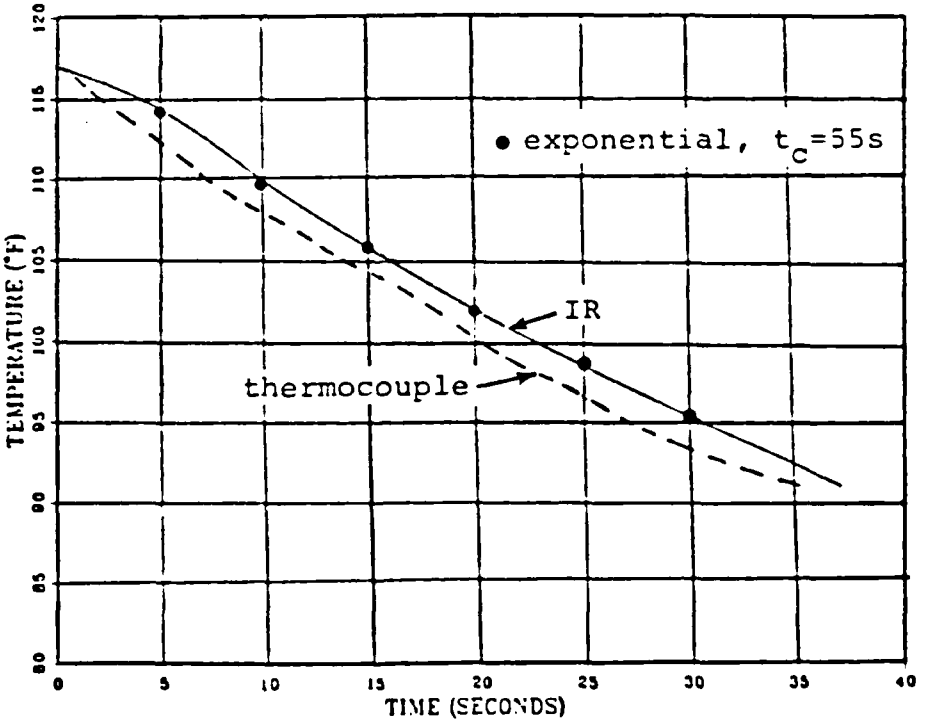

Figure 10. Temperature-time responses meaured by thermocouple and IR sensor; 306 ft/s freestream speed.

thermocouple location. Figure 10 shows typical time histories of these temperatures, indicating the agreement of the temperature decay rates with expected exponential form. In the table below, results are shown for both sets of measurements. The experimental uncertainty for the two representative speeds shown was on the order of 2 Btu/hr-ft^2-R [39], indicating remarkably good agreement between the two methods -- virtually

Tunnel Speed ft/sec	Film Coefficient, h Btu/hr-ft^2-R	
	Thermocouple	IR System
200	27.5 - 33.2	27.7 - 33.5
306	41.0 - 42.7	39.9 - 41.8

identical within experimental uncertainty. The theoretical flat plate estimates for the film coefficient are 22 and 28 Btu/hr-ft^2-R for 200 and 306 ft/s, respectively, on the assumption of laminar flow. In both cases, this assumption is marginal, and the results indicate that turbulent or transitional flow probably existed at the location of the measurement. (This conclusion is further supported by the increased deviation at the higher speed.)

These tests served as a valuable learning experience. In hindsight, after encountering and working-out many experimental bugs, it seems probable that the planned initial testing in the supersonic wind tunnel was ill-conceived. In addition, these results validate the application of the transient method using IR thermography.

It is important to note that the measurements given above correspond to conditions at a particular point on the wedge -- the location of the thermocouple in this case. Further testing, with the cursor positioned at other points, would allow the development of a complete heat transfer map of the wedge surface. However, viewing of the thermal behavior of the entire wedge surface showed that the transient isotherm variation was essentially uniform over a large portion of the surface (with the exception of narrow bands in the three-dimensional boundary layer regions near the sidewalls). Thus it may be deduced that the values determined above, at the thermocouple location, are representative of conditions over a major portion of the wedge surface. The ability to make such observations, which might otherwise require the use of hundreds of simultaneous point measurements, is a significant virtue of the IR thermography method.

IR Thermography of a Jet Vane. The advantages of the IR thermography method are especially dramatic when it is used to view the thermal behavior of complicated configurations leading to flow effects that are well beyond exact analytical capabilities. Such is the case for the jet vane, and some preliminary testing was done in order to demonstrate the method.

The vane tested, shown mounted in the tunnel in Fig. 11, was constructed of copper-impregnated tungsten with an estimated volume-to-surface area ratio of about 1.5×10^{-4} ft. Thus, even though an exact value could not be calculated, the

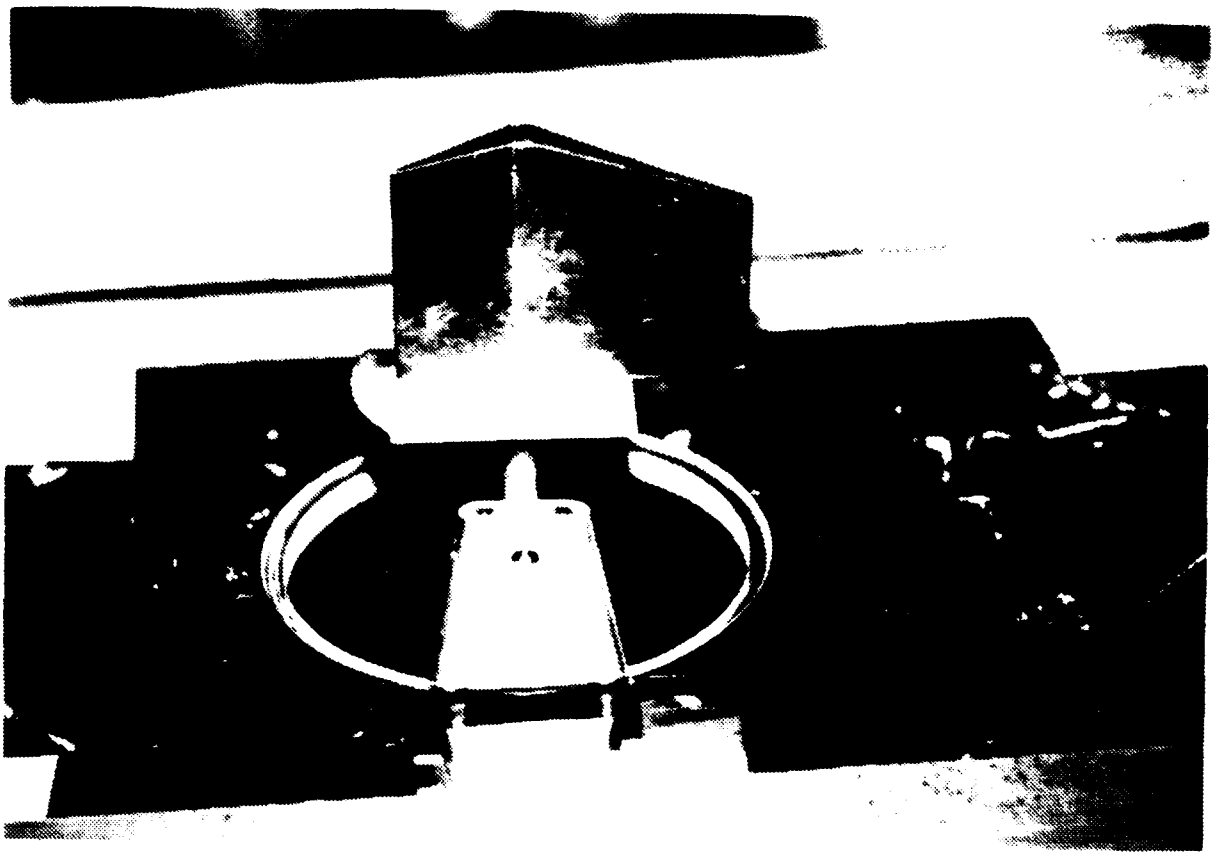

Figure 11. Photograph of jet vane model mounted in subsonic wind tunnel.

Biot number was well within the acceptable range. This was verified by the exponential temperature responses obtained in the tests. At 200 ft/s, the midspan heat transfer coefficient was measured to be 41.5 Btu/hr-ft^2-R, while a measurement at the vane/baseplate intersection indicated a 32% increase over this value.

By simply viewing the time history of the thermal response of the vane, it was possible to note the expected high heat transfer rates at the vane leading and trailing edges. Other areas of high heat transfer were noted just downstream of the ridge of the vane, particularly near the tip. In other

areas, the heat transfer appeared to be more-or-less uniform. Again, these tests proved the effectiveness of the method and indicated many possibilities for future research using this application of IR thermography. Further details regarding these tests, including color prints of the IR images, may be found in Spence [39].

CONCLUSION

Preliminary work has been carried out to develop the capability to model the heat transfer processes encountered by jet vane thrust vector control systems. Computational modeling has begun using the PHOENICS code. The initial configurations investigated were two-dimensional approximations to the NWC jet vane geometry. Two separate leading edge geometries have been investigated: a sharp wedge leading edge; and a rounded nose wedge. The results from these calculations indicate that the leading edge geometry has a very strong effect on the skin friction and surface heat transfer over the whole body. Work is continuing to investigate the effects of the leading edge geometry on the surface skin friction and heat transfer. It is believed that these effects stem from the complex shock wave boundary layer interaction near the leading edge. To carry out this investigation the latest version of the PHOENICS code (PHOENICS 84) is being procured. This version of PHOENICS will allow more precise modeling of various leading edge geometries as well as the modeling of three dimensional flow configurations.

In support of the computational modeling effort an experimental program has also been initiated. The purpose of this effort is to obtain confirmation of the computational results. The initial experimental work has been carried out in the subsonic wind tunnel and it is intended to continue the experimental work in the NPS supersonic wind tunnel.

REFERENCES

1. National Aeronautics and Space Administration, "Solid Rocket Thrust Vector Control," NASA SP-8114, Lewis Research Center, Cleveland, OH, Dec., 1974.

2. Kampa, D., A. Weiss, R.H. Schmucker, "Material Problems in Jet Vane Thrust Vector Control Systems," AGARD-CP-259.

3. Wirtz, D.P., "Preliminary Design and Performance Estimate of a Jet Vane Attachment in a Rocket Nozzle," internal memorandum 45701/DPW:cad, Reg. 45701-242-73, Naval Weapons Center, CA, 4 June, 1973.

4. Ziebland, H. and R. C. Parkinson, "Heat Transfer in Rocket Engines," AGARD-AG-148-71, AGARD, Sept., 1971.

5. Holman, J. P., Heat Transfer, 4th ed., McGraw-Hill Book Co., New York, 1976.

6. Chemical Propulsion Information Agency, Thrust Vector Control for Tactical Missiles -- A Bibliography, Rep. No. LS84-23, CPIA, APL, Laurel, Md., Oct., 1984

7. Hankey, W. L., and M. S. Holden, "Two-Dimensional Shock Wave-Boundary Layer Interactions in High Speed Flows," AGARD-AG-203, AGARD, June, 1975.

8. Kaye, Joseph, "Survey of Friction Coefficients, Recovery Factors, and Heat-Transfer Coefficients for Supersonic Flow," J. Aero. Sci., Feb., 1954.

9. Eckert, E. R. G., "Engineering Relations for Heat Transfer and Friction in High-Velocity Laminar and Turbulent Boundary-Layer Flow Over Surfaces with Constant Pressure and Temperature," in Recent Advances in Heat Transfer, McGraw-Hill, New York, 1961.

10. van Driest, E. R., "The Problem of Aerodynamic Heating," Aero. Eng. Review, Oct., 1956.

11. ----, "Convective Heat Transfer in Gases," in High Speed Aerodynamics and Jet Propulsion, v. V, Princeton Univ. Press, Princeton, 1959.

12. Summerfield, M., "The Liquid Propellant Rocket Engine," in High Speed Aerodynamics and Jet Propulsion, v. XII, Princeton Univ. Press, Princeton, 1959.

13. Shapiro, A. H., The Dynamics and Thermodynamics of Compressible Fluid Flow, v.II, Ronald Press, New York, 1954.

14. Hung, F. T., S. N. Greenschlag, and C. A. Scottoline, "Shock-Wave-Boundary-Layer Interaction Effects on Aerodynamic Heating," J. Spacecraft, v.14, no.1, Jan. 1977.

15. Back, L. H., and R. F. Cuffel, "Changes in Heat Transfer from Turbulent Boundary Layers Interacting with Shock Waves and Expansion Waves," AIAA Journal, v.8, no.10, Oct. 1970.

16. Han Yinda, "Experimental Research on Separation, Heat Transfer and Ablation of the Model of Flat Plate in Supersonic Turbulent Flow," AIAA/ASME 4th Joint Thermophysics and Heat Transfer Conference, Paper AIAA-86-1237, Boston, June 2-4, 1986.

17. Mayer, E., and R. Prickett, "Rocket Plume Impingement Heat Transfer on Plane Surfaces," AIAA/ASME 4th Joint Thermophysics and Heat Transfer Conference, Paper AIAA-86-1321, Boston, June 2-4, 1986.

18. Whitaker, K. W., and C. Ostowari, "Heat Transfer Behavior with Convex Target Surfaces," AIAA/ASME 4th Joint Thermophysics and Heat Transfer Conference, Paper AIAA-86-1236, Boston, June 2-4, 1986.

19. Sedney, R. and C. W. Kitchens, Jr., "Separation ahead of Protuberances in Supersonic Turbulent Boundary Layers," AIAA Journal, v.15, no.4, April, 1977.

20. Datis, A., B. G. Broach, and H. H. Yen, "Heat Transfer in the Vicinity of Two-Dimensional Protuberances," J. Spacecraft, v.1, no.6, Nov.-Dec., 1964.

21. Motwani, D. G., U. N. Gaitonde and S. P. Sukhatme, "Heat Transfer from Rectangular Plates Inclined at Different Angles of Attack and Yaw to an Air Streem," J. Heat Transfer, v.107, May, 1985.

22. Peyret, R. and Taylor, T. D., Computational Methods for Fluid Flow, Springer-Verlag, New York, 1983.

23. Patankar, S. V., Numerical Heat Transfer and Fluid Flow, Hemisphere Publishing Corp. (McGraw-Hill Book Co.), New York, 1980.

24. Jaluria, Y. and Torrence, K., Computational Heat Transfer, Hemisphere Publishing Corp., Washington, 1986.

25. MacCormack, R. W. and Lomax, H., "Numerical Solution of Compressible Viscous Flows," in Annual Review of Fluid Mechanics, v. 11, Annual Reviews, Inc., Palo Alto, CA, 1979.

26. Book, D. L., (editor), Finite Difference Techniques for Vectorized Fluid Dynamics Calculations, Springer-Verlag, New York, 1981.

27. Gunton, M. C., Rosten, H. I., Spalding, D. B., and Tatchell, D. G., PHOENICS an Instruction Manual, Concentration Heat and Momentum, Ltd., London, 1983.

28. Leitner, A., Thrust Vector Control, Heat Transfer Modeling, Contractor Report, Naval Postgraduate School, NPS69-86-005, Monterey, CA, 1986.

29. Yukselen, A.,"Heat Transfer Modeling of Thrust Vector Control Systems", Thesis for Master of Science, Naval Postgraduate School, Monterey, CA, March, 1986.

30. High Speed Problems of Aircraft and Experimental Methods, High Speed Aerodynamics and Jet Propulsion, v.VIII, ed. A. F. Donovan, et al., Princeton Univ. Press, Princeton.

31. Eber, G. R., "Wall Temperature Determination," in High Speed Aerodynamics and Jet Propulsion, vIX, Princeton Univ. Press, Princeton, 1954.

32. Burbank, P. G., and B. L. Hodge, "Distribution of Heat Transfer on a 10x Cone at Angles of Attack from 0x to 15x for Mach Numbers of 2.49 to 4.65 and a Solution to the Heat Transfer Equation that Permits Complete Machine Calculations," MEMO 6-4-59L, NASA, Washington, June, 1959.

33. Williams, S. D., and D. M. Curry, "An Analytical and Experimental Study for Surface Heat Flux Determination," J. Spacecraft, v.14, no.10, Oct., 1977.

34. Mehta, R. C., "Estimation of Heat-Transfer Coefficient in a Rocket Nozzle," AIAA Journal, v.19, no.8, Aug., 1981.

35. Raynaud, M., "Combination of Methods for the Inverse Heat Conduction Problem with Smoothing Filters," AIAA/ASME 4th JointThermophysics and Heat Transfer Conference, Paper AIAA-86-1243, Boston, June 2-4, 1986.

36. "Equations, Tables, and Charts for Compressible Flow," Ames Research Staff, Report 1135, NACA, Washington, 1953.

37. Hughes Aircraft Company, PROBEYE Thermal Video System Series 4000 Operating Manual, Industrial Products Division, Sept., 1983.

38. Eastman Kodak Company, Kodak IRTRAN Infrared Optical Materials, Pub. no. U-72, Kodak Apparatus Div., 1981.

39. Spence, T. M., "Applications of Infrared Thermography in Convective Heat Transfer," Thesis for Master of Science, Naval Postgraduate School, Monterey, March, 1986.

INITIAL DISTRIBUTION LIST

		No. Copies
1.	Library, Code 0142 Naval Postgraduate School Monterey, CA 93943	2
2.	Research Administration Code 012 Naval Postgraduate School Monterey, CA 93943	1
3.	Department Chairman, Code 69 Department of Mechanical Engineering Naval Postgraduate School Monterey, CA 93943	1
4.	Professor Matthew D. Kelleher, Code 69Kk Department of Mechanical Engineering Naval Postgraduate School Monterey, CA 93943	2
5.	Professor Robert H. Nunn, Code 69Nn Department of Mechanical Engineering Naval Postgraduate School Monterey, CA 93943	2
6.	Professor David Salinas, Code 69Sa Department of Mechanical Engineering Naval Postgraduate School Monterey, CA 93943	1
7.	A. Leitner Visiting Research Associate Department of Mechanical Engineering Naval Postgraduate School Monterey, CA 93943	3
8.	Dr. R. Dillinger Naval Weapon Center China Lake, CA 93555	1
9.	Dr. C. Porter Naval Weapon Center China Lake, CA 93555	1
10.	Mr. A. Danielson Naval Weapon Center China Lake, CA 93555	1

11. Defense Technical Information Center 1
Cameron Station, VA 22314

END

2-87

DTIC